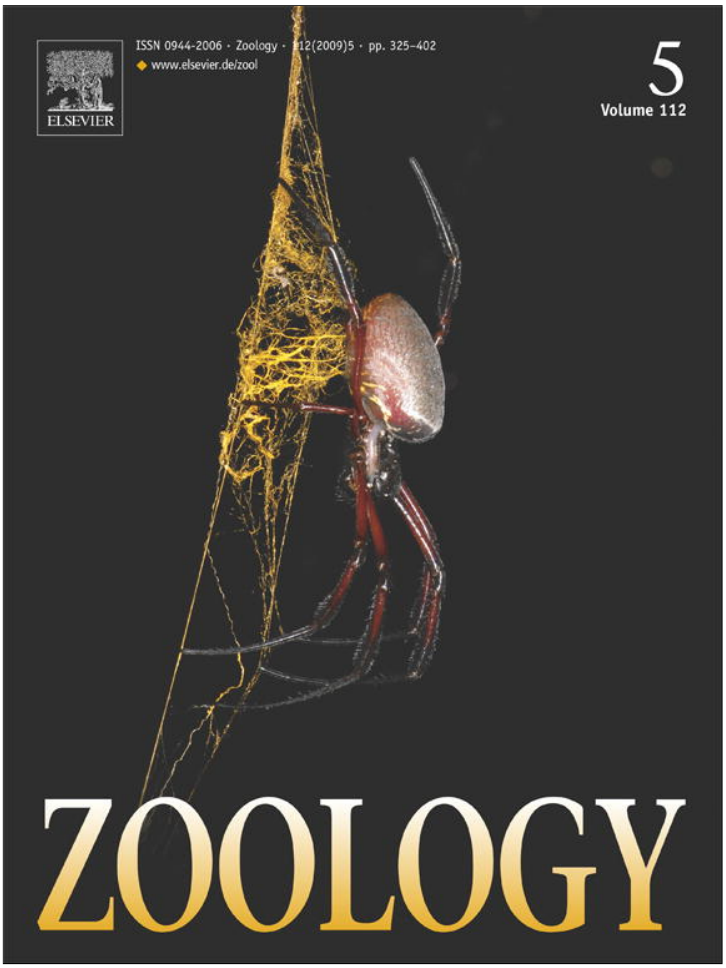

Available online at www.sciencedirect.com
ScienceDirect
Zoology 112 (2009) 351–361
ZOOLOGY
www.elsevier.de/zool

Scaling of feeding biomechanics in the horn shark *Heterodontus francisci*: ontogenetic constraints on durophagy

Matthew A. Kolmann, Daniel R. Huber*

Department of Biology, University of Tampa, 401 W. Kennedy Blvd., Box U, Tampa, FL 33606, USA

Received 10 September 2008; received in revised form 31 October 2008; accepted 13 November 2008

Abstract

Organismal performance changes over ontogeny as the musculoskeletal systems underlying animal behavior grow in relative size and shape. As performance is a determinant of feeding ecology, ontogenetic changes in the former can influence the latter. The horn shark *Heterodontus francisci* consumes hard-shelled benthic invertebrates, which may be problematic for younger animals with lower performance capacities. Scaling of feeding biomechanics was investigated in *H. francisci* ($n = 16$, 19–59 cm standard length (SL)) to determine the biomechanical basis of allometric changes in feeding performance and whether this performance capacity constrains hard-prey consumption over ontogeny. Positive allometry of anterior (8–163 N) and posterior (15–382 N) theoretical bite force was attributed to positive allometry of cross-sectional area in two jaw adducting muscles and mechanical advantage at the posterior bite point (0.79–1.26). Mechanical advantage for anterior biting scaled isometrically (0.52). Fracture forces for purple sea urchins *Strongylocentrotus purpuratus* consumed by *H. francisci* ranged from 24 to 430 N. Comparison of these fracture forces to the bite force of *H. francisci* suggests that *H. francisci* is unable to consume hard prey early in its life history, but can consume the majority of *S. purpuratus* by the time it reaches maximum size. Despite this constraint, positive allometry of biting performance appears to facilitate an earlier entry into the durophagous niche than would an isometric ontogenetic trajectory. The posterior gape of *H. francisci* is significantly smaller than the urchins capable of being crushed by its posterior bite force. Thus, the high posterior bite forces of *H. francisci* cannot be fully utilized while consuming prey of similar toughness and size to *S. purpuratus*, and its potential trophic niche is primarily determined by anterior biting capacity.

Keywords: Bite force; Cartilaginous fishes; Durophagy; Feeding ecology; Trophic constraints

Introduction

Organismal performance changes over ontogeny as the musculoskeletal systems underlying animal behavior change in relative size and shape. Vertebrates generally exhibit positive allometry of feeding performance (bite force, jaw velocity) over ontogeny, such that adults have relatively higher performance than juveniles (Herrel and Gibb, 2006). These allometric growth patterns are often associated with dietary shifts and niche partitioning because increased performance facilitates the consumption of functionally difficult prey (hard, tough, large, etc.), that other species, or younger members of the same species, are incapable of consuming (Hernandez and

*Corresponding author. Tel.: +1 813 253 3333; fax: +1 813 258 7496.
E-mail address: dhuber@ut.edu (D.R. Huber).

0944-2006/$ - see front matter © 2009 Elsevier GmbH. All rights reserved.
doi:10.1016/j.zool.2008.11.002

Motta, 1997; Aguirre et al., 2003; Herrel and O'Reilly, 2006). Thus, positive allometry of feeding performance assists predators in overcoming the functional constraints imposed by their prey and may confer a competitive advantage over isometric ontogenetic trajectories, facilitating access to exclusive trophic resources earlier in life.

Prey hardness is a significant constraint on feeding ecology. Those taxa capable of generating sufficient bite forces to consume hard prey benefit from reduced competition owing to the lower performance capacities of sympatric species. Accordingly, high bite forces are often associated with increased hard-prey consumption and reduced trophic diversity (niche specialization) among species and over an individual species' ontogeny (Wainwright, 1988; Hernandez and Motta, 1997; Clifton and Motta, 1998; Wyckmans et al., 2007). High bite forces also increase the rate of net energy intake by increasing prey handling efficiency. Thus, the selective pressure for ontogenetic growth patterns facilitating high-performance biting is apparent (Verwaijen et al., 2002; van der Meij et al., 2004; Herrel and Gibb, 2006). As hardness is strongly correlated with prey size, the physical dimensions of prey items pose a potential constraint on trophic ecology as well (Currey, 1980; Keast, 1985; Wainwright, 1987; Aguirre et al., 2003; Korff and Wainwright, 2004).

The manner in which durophagous cartilaginous fishes overcome prey hardness as a constraint on feeding ecology is particularly intriguing given that benthic invertebrates are often orders of magnitude harder than the hyaline cartilage comprising the chondrichthyan endoskeleton (Wainwright et al., 1976; Currey, 1980; Summers and Long, 2006; Wroe et al., 2008). Durophagy has evolved numerous times among cartilaginous fishes and is facilitated by a suite of convergently evolved morphological characteristics including robust, high-leverage jaws, molariform dentition, and hypertrophied jaw adductors (Summers, 2000; Huber et al., 2005, 2008). Sustained adductor contraction, force amplification through asymmetrical biting, and cyclical loading of prey items have been identified as behavioral correlates of durophagy in cartilaginous fishes as well (Summers, 2000; Wilga and Motta, 2000; Huber et al., 2005). Collectively, these traits facilitate high-performance biting (i.e. high bite force) which is key to accessing the relatively competitor-free durophagous niche (Kiltie, 1982; Wainwright, 1988; Clifton and Motta, 1998).

While the functional basis of durophagy in cartilaginous fishes has become understood in recent years, the manner in which ontogenetic changes in their feeding mechanisms affect biting performance and constrain feeding ecology is largely unknown. Therefore, the relationship between scaling of feeding biomechanics, feeding ecology, and trophic constraints was investigated in the horn shark *Heterodontus francisci* (Girard 1855). *H. francisci* is a nocturnal forager of benthic echinoderms, mollusks, and crustaceans. Hard prey comprises approximately 94% of its diet, which it captures via a bimodal suction-crushing mechanism (Strong, 1989; Segura-Zarzosa et al., 1997; Edmonds et al., 2001; Huber et al., 2005). The specific objectives of this study were to (1) determine scaling patterns of feeding biomechanics in *H. francisci* over ontogeny; (2) determine the fracture properties of a primary prey item of *H. francisci*, the purple sea urchin *Strongylocentrotus purpuratus*; and (3) identify ontogenetic constraints on the feeding ecology of *H. francisci* by comparing its bite force to the fracture properties of *S. purpuratus* with respect to urchin size. We hypothesized that *H. francisci* will exhibit positive allometry of bite force, which will facilitate entry into the durophagous trophic niche early in its life history.

Materials and methods

Cranial morphology and biomechanics

Cranial measurements were taken from 16 *H. francisci* (19–59 cm standard length (SL)) obtained from fisheries by-catch and museum collections (MCZ-392, MCZ-491, and MCZ-155798 from the Harvard University Museum of Comparative Zoology; CMNFI 1974-0217.1 from the Canadian Museum of Nature). By-catch specimens were freshly frozen after capture and museum specimens were stored in 70% ethanol. All dissection protocols were performed in accordance with the Institutional Animal Care and Use Committee of the University of South Florida (IACUC #1882).

Standard length (distance from tip of the snout to base of the caudal fin), maximum anterior gape (distance between the tips of the lower and upper jaws with the lower jaw maximally depressed and the upper jaw not protruded), prebranchial length (distance from tip of the snout to the first gill slit), head height (distance between the dorsal and ventral margins of the head), and head width (distance between the lateral margins of the head) at the first gill slit were recorded for each specimen (raw data see the Appendix at doi:10.1016/j.zool.2008.11.002). Maximum posterior gape was estimated through iterative use of the law of sines:

$$\frac{a}{\sin A} = \frac{b}{\sin B}$$

where a is the maximum gape distance, A is the gape angle, b is the length of the lower jaw to either the anterior or posterior bite point, and B is the angle of the upper jaw relative to the vertical axis orthogonal to the longitudinal axis of the body. B was first estimated for each specimen using the following: $a =$ maximum

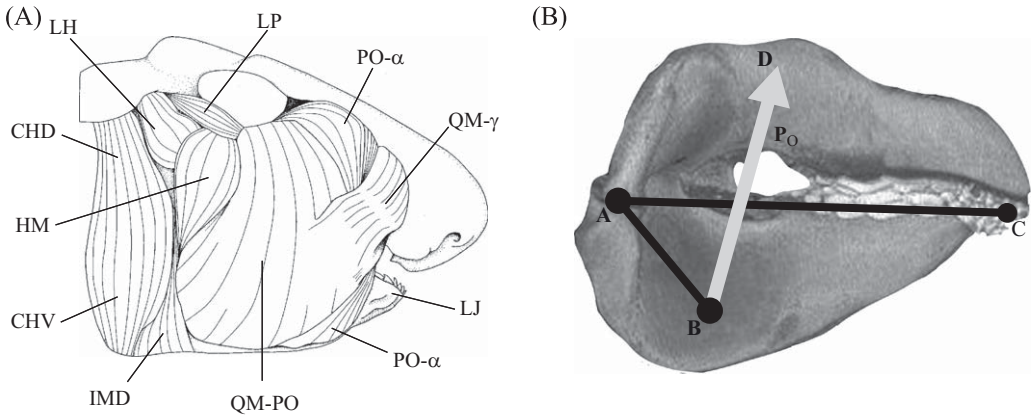

Fig. 1. (A) Right lateral view of the cranial musculature of *H. francisci*. CHD, dorsal hyoid constrictor; CHV, ventral hyoid constrictor; HM, hyomandibulo-mandibularis; IMD, intermandibularis; LH, levator hyomandibularis; LJ, lower jaw; LP, levator palatoquadrati; QM–PO, quadratomandibularis–preorbitalis complex; PO-α, preorbitalis-α, QM-γ, quadratomandibularis-γ. (B) Right lateral view of the jaws of *H. francisci* indicating measurements used in calculating mechanical advantage. A–B, resolved in-lever for jaw adduction; A–C, out-lever; B–D, adductive muscle force vector; P_O, maximum tetanic tension. Images modified from Huber et al. (2005).

anterior gape; A = gape angle of 22° from kinematic analyses (D.R. Huber, unpublished data); b = length of the lower jaw to the anterior bite point (see below). Maximum posterior gape distance (a) was then estimated using the following: A = gape angle of 22°; b = length of the lower jaw to the posterior bite point (see below); B = angle calculated in iteration #1.

The three muscles involved in jaw adduction in *H. francisci* are the quadratomandibularis–preorbitalis complex (QM–PO), preorbitalis-α (PO-α), and quadratomandibularis-γ (QM-γ) (Fig. 1A). The positions of the origins and insertions of each muscle, as well as the jaw joint and anterior and posterior margins of the functional tooth row on the lower jaw (anterior and posterior bite points) were determined with respect to a 3D coordinate system originating at the tip of the snout. Each of the muscles was unilaterally excised and sectioned through its center of mass perpendicular to the principal muscle fiber direction. Cross-sections were photographed with a Panasonic Lumix DMC-FZ50 digital camera and areas were measured using Sigma Scan Pro 4.01 (SYSTAT Software, Inc., Point Richmond, CA, USA). The theoretical maximum tetanic tension (P_O) produced by each muscle was then estimated by multiplying its cross-sectional area (A_{CS}) by the specific tension (T_S) of elasmobranch white muscle (289 kN m^{-2}) (Lou et al., 2002):

$$P_O = A_{CS} T_S$$

In-lever distances for each muscle were determined from the three-dimensional coordinates of their respective insertions on the lower jaw and the jaw joint, and a weighted average of the in-levers based on the forces produced by each muscle was used to determine a resultant in-lever. Out-lever distances to the anterior and posterior bite points were determined from the three-dimensional coordinates of these points and the jaw joint as well. Mechanical advantages for anterior and posterior biting were then calculated by dividing the resultant in-lever by the out-lever distances to the anterior and posterior bite points (Fig. 1B).

Force vectors for each muscle were generated based on their theoretical maximum tetanic tensions and three-dimensional coordinates of origin and insertion. These vectors were reflected about the X–Y plane to represent forces generated bilaterally by the jaw adducting musculature. Theoretical maximum bite forces at the anterior and posterior bite points were calculated by summation of bending moments generated on the lower jaw by the jaw adducting musculature about the jaw joints (Mathcad 11.1 software; Mathsoft, Inc., Cambridge, MA, USA). The static equilibrium conditions for the forces acting on the lower jaw (F_{LJ}) were:

$$\sum F_{LJ} = F_{JR} + F_{QM-PO} + F_{QM\text{-}\gamma} + F_{PO\text{-}\alpha} + F_B = 0$$

where F_B is the bite reaction force from a prey item, F_{JR} is the jaw joint reaction force, $F_{PO\text{-}\alpha}$ is the force generated by the preorbitalis-α, F_{QM-PO} is the force generated by the quadratomandibularis–preorbitalis complex, and $F_{QM\text{-}\gamma}$ is the force generated by the quadratomandibularis-γ. Joint reaction forces maintain the static equilibrium of feeding mechanisms by balancing the moments acting upon the jaws via their associated musculature and contact with prey items.

Failure forces of prey

Purple sea urchins *S. purpuratus* ($n = 30$) from southern California waters inhabited by *H. francisci* were obtained from a commercial distributor (Marine Research and Educational Products, Carlsbad, CA,

USA) and kept in 38 l aquaria at 15 °C and 30 ppt. The height, diameter, and mass (excluding spines) of all *S. purpuratus* were recorded, after which they were subjected to axial compression tests in a MTS Mini Bionix 858 hydraulic material testing system (MTS, Eden Prairie, MN, USA). All compression tests were performed on live urchins, which were crushed along the dorso-ventral axis between *H. francisci* jaws that were removed from a 34.5 cm SL specimen, embedded in epoxy, affixed to steel plates, and mounted to the MTS system. Forces (N) at which the *S. purpuratus* tests underwent catastrophic failure were recorded. The crushing protocol was consistent with observations of urchin consumption by *H. francisci*, wherein the lateral margin (~25%) of an *S. purpuratus* test is grasped between the jaws and crushed, after which test fragments are manipulated and soft tissues are transported through the oropharyngeal cavity via inertial suction (Strong, 1989). Size distributions for *S. purpuratus* throughout waters inhabited by *H. francisci* were obtained from Ebert (1968) and Morris et al. (1980) to place the present data in the context of the potential prey spectrum represented by *S. purpuratus*.

Statistics

Cranial morphometrics, muscle cross-sectional areas, lever distances, mechanical advantages, and theoretical bite forces were log transformed and linearly regressed against log transformed standard length. Scaling relationships of these variables with respect to standard

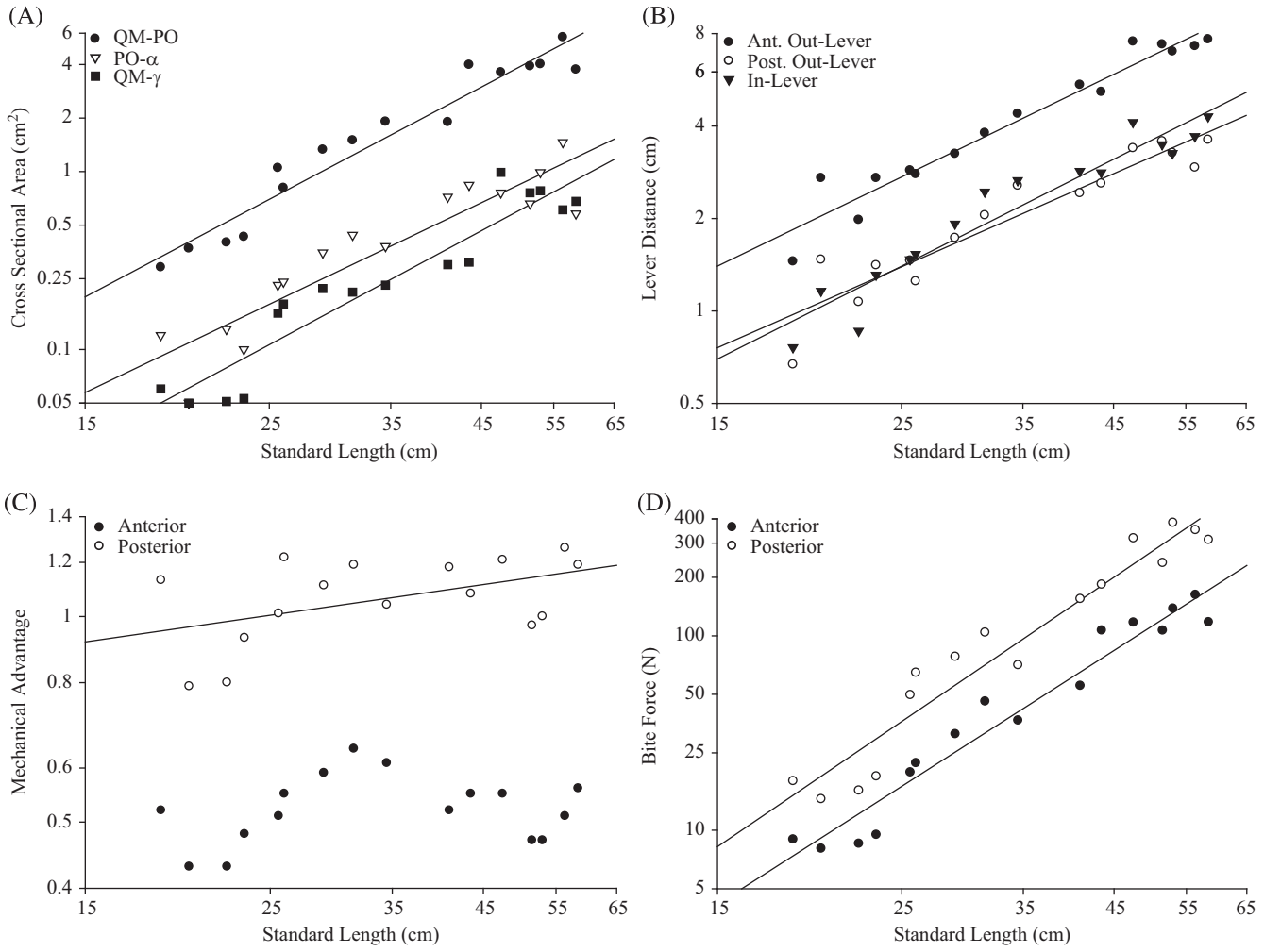

Fig. 2. Ontogenetic changes in biomechanical variables with respect to standard length (SL) in *H. francisci* plotted on logarithmic axes: (A) jaw adductor cross-sectional areas (CSA) ($\log$ QM–PO CSA $= 2.48 \log$ SL$-\log 3.62$, $\log$ PO-α CSA $= 2.22 \log$ SL$-\log 3.88$, $\log$ QM-γ CSA $= 2.53 \log$ SL$-\log 4.51$). (B) In-lever ($\log L_I = 1.37 \log$ SL$-\log 1.77$), anterior out-lever ($\log$ ant $L_O = 1.31 \log$ SL$-\log 1.40$), and posterior out-lever ($\log$ post $L_O = 1.19 \log$ SL$-\log 1.51$) distances for jaw adduction. (C) Anterior ($\log$ ant MA $= 0.06 \log$ SL$-\log 0.38$) and posterior ($\log$ post MA $= 0.17 \log$ SL$-\log 0.24$) mechanical advantage (MA) for jaw adduction. (D) Anterior ($\log$ ant BF $= 2.71 \log$ SL$-\log 2.61$) and posterior ($\log$ post BF $= 2.91 \log$ SL$-\log 2.51$) theoretical maximum bite force (BF). See Table 1 for additional statistical information.

length were assessed with a Student's *t*-test by comparing the slope of a given variable to the appropriate isometric slope (mechanical advantage = 0; morphometrics and lever distances = 1; areas and forces = 2). Scaling of muscle areas and forces with respect to head dimensions, and of *S. purpuratus* failure forces with respect to urchin height, diameter, and mass were also performed in this manner.

The ability to resist loading is a function of area. Therefore, *S. purpuratus* failure forces were compared to an isometric slope of 2 with respect to urchin height and diameter (linear functions), and 0.67 with respect to mass (cubic function). Linear regression was used to determine the predictive ability of cranial morphometrics with respect to anterior and posterior theoretical bite forces as well.

Based on the relationship between *S. purpuratus* test height and failure force, theoretical maximum anterior and posterior bite forces for *H. francisci* were used to predict the largest *S. purpuratus* each shark in our sample was capable of crushing with an anterior or posterior bite. To determine the absolute capacity of *H. francisci* to consume hard prey such as *S. purpuratus*, anterior and posterior bite forces and predicted maximum urchin heights were also estimated for the smallest (13 cm SL) and largest (93 cm SL) *H. francisci* on record (Compagno, 2001). To determine whether anterior and posterior gape distances constrain the size of *S. purpuratus* consumed by *H. francisci*, anterior and posterior gape distances and predicted *S. purpuratus* heights were log transformed and regressed against standard length. The slopes and *y*-intercepts for gape distance and predicted urchin height at each bite point were then compared using Student's *t*-tests. Behavioral observations indicate that *H. francisci* does not draw whole urchin tests into its mouth prior to crushing. Rather, it grasps and crushes the lateral margin (~25%) of the test, thereby making urchin height, not width, the immediate dimension it must contend with during feeding. Thus, urchin width/gape width relationships were not analyzed. Linear regressions were performed in SigmaStat 2.03 (SYSTAT Software, Inc., Point Richmond, CA, USA) and Student's *t*-tests were performed manually ($p = 0.05$).

Results

Scaling of feeding biomechanics

The cross-sectional areas of the QM–PO and QM-γ scaled with positive allometry over ontogeny in *H. francisci*, while that of PO-α scaled isometrically (Fig. 2A and Table 1). At all sizes the QM–PO had the largest cross-sectional area, contributing 71% of the adductive force, followed by PO-α (18%) and QM-γ (11%). The in-lever for jaw adduction and the out-lever to the anterior bite point both scaled with positive allometry while the posterior out-lever scaled isometrically (Fig. 2B and Table 1). Allometry of the adductive in-lever and anterior out-lever cancelled each other out (slopes = 1.37 and 1.31, respectively) such that mechanical advantage for anterior biting scaled isometrically (mean = 0.52). However, posterior mechanical advantage exhibited positive allometry, ranging from 0.79 to 1.26, by virtue of the relative growth of the adductive in-lever and posterior out-lever (Fig. 2C and Table 1).

Table 1. Scaling analyses of morphometric and biomechanical variables with respect to standard length (SL) in the feeding mechanism of *H. francisci* ($\log y = b \log \mathrm{SL} + \log a$).

Variable	Isometric slope	Slope	*y*-intercept	r^2	$t_{(0.05(1),\ 14)}$	*p*
Anterior gape (cm)	1	1.63	−2.13	0.942	6.052	**<0.001**
Posterior gape (cm)	1	1.50	−2.26	0.920	4.239	**<0.001**
Prebranchial length (cm)	1	1.28	−1.18	0.934	3.104	**0.005**
Head height (cm)	1	1.15	−1.07	0.945	1.966	**0.033**
Head width (cm)	1	1.06	−0.83	0.914	0.690	0.251
QM–PO cross-sectional area (cm^2)	2	2.48	−3.62	0.940	2.855	**0.006**
PO-α cross-sectional area (cm^2)	2	2.24	−3.88	0.844	0.932	0.184
QM-γ cross-sectional area (cm^2)	2	2.53	−4.51	0.888	2.211	**0.022**
Resultant in-lever (cm)	1	1.37	−1.77	0.918	3.377	**0.002**
Anterior out-lever (cm)	1	1.31	−1.40	0.942	3.583	**0.001**
Posterior out-lever (cm)	1	1.19	−1.51	0.882	1.598	0.066
Anterior mechanical advantage	0	0.06	−0.38	0.043	0.798	0.219
Posterior mechanical advantage	0	0.17	−0.24	0.224	2.017	**0.023**
Anterior bite force (N)	2	2.71	−2.61	0.949	4.205	**< 0.001**
Posterior bite force (N)	2	2.91	−2.51	0.928	4.195	**< 0.001**

All initial regressions from which slopes, *y*-intercepts, and r^2 values were obtained were significant at $p \leq 0.025$ with the exception of anterior mechanical advantage. Bold numbers indicate statistically significant *p*-values.

Owing to allometric increases in the forces produced by QM–PO and QM-γ and posterior mechanical advantage, both anterior (8–163 N) and posterior (15–382 N) theoretical bite force scaled with positive allometry (Fig. 2D and Table 1).

Anterior and posterior gape, prebranchial length, and head height all scaled with positive allometry in *H. francisci*. Head width was the only cranial morphometric to exhibit an isometric growth pattern (Table 1). All cranial morphometrics were highly related to theoretical bite force, with head width as the strongest predictor of anterior bite force ($r^2 = 0.940$) and head height as the strongest predictor of posterior bite force ($r^2 = 0.914$) (Table 2). The vertical (*Y*-axis) vector components of the jaw adducting muscle forces are the principal effectors of bite force generation during static biting. *Y*-axis vector components for QM–PO and QM-γ scaled with positive allometry relative to standard length, and those of all three muscles scaled isometrically to head height, indicating a strong relationship between head height and adductive force generation in *H. francisci* (Table 3). Additionally, the cross-sectional area of QM–PO scaled to head width with positive allometry, suggesting an internal reorganization of the feeding mechanism relative to the isometric increase in head width (Table 3).

Table 2. Results of regression analyses to determine the predictive ability of cranial morphometrics with respect to bite force in *H. francisci* ($\log Y = b \log x + \log a$).

Variable	Regression equation	r^2
Prebranchial length (cm)	ABF = 1.994 PBL + 0.045	0.873
Head height (cm)	ABF = 2.295 HH + 0.019	0.930
Head width (cm)	ABF = 2.462 HW − 0.363	0.940
Prebranchial length (cm)	PBF = 2.111 PBL + 0.311	0.851
Head height (cm)	PBF = 2.440 HH + 0.276	0.914
Head width (cm)	PBF = 2.592 HW − 0.109	0.906

ABF = anterior bite force; HH = head height; HW = head width; PBF = posterior bite force; PBL = prebranchial length.

Failure forces of prey

The failure forces of *S. purpuratus* tests ranged from 24 to 430 N and showed the strongest relationship to urchin mass (2.1–132.6 g, $r^2 = 0.809$), as compared to test diameter (1.8–7.2 cm, $r^2 = 0.788$) or test height (0.8–3.5 cm, $r^2 = 0.779$) (Fig. 3). Failure force scaled isometrically relative to urchin mass, although it scaled with negative allometry relative to test diameter and height (Table 4).

Ontogenetic constraints on feeding ecology

Based on the relationship between *S. purpuratus* height and failure force (log height = 0.461 log force–0.706), it was predicted that urchins ranging from 0.51 to 2.05 cm could be crushed by the anterior bite force of the *H. francisci* in our sample, and from 0.67 to 3.04 cm using posterior bite force (Fig. 4). The largest of these urchins (2.05, 3.04 cm) represent only 40% and 68% of the size range of *S. purpuratus* (0.6–4.2 cm test height), respectively. Using the relationship between theoretical bite force and standard length (Table 1) it was predicted that *H. francisci* can generate anterior and posterior bite forces ranging from 3 to 530 N and 5 to 1653 N, respectively, over its entire size range (13–93 cm SL). Relating these values to urchin failure forces suggests that *H. francisci* cannot consume *S. purpuratus* (minimum 0.6 cm test height) with anterior biting until 21 cm SL, based solely on its anterior bite force capacity. If posterior gape is not a limiting factor, *H. francisci* can begin consuming *S. purpuratus* with posterior biting at 17 cm SL. Thus, *H. francisci* is prevented from

Table 3. Scaling analyses of *y*-axis force vector components and cross-sectional areas of jaw adducting muscles in *H. francisci* with respect to standard length and cranial morphometrics ($\log y = b \log x + \log a$).

Dependent variable	Independent variable	Isometric slope	Slope	*y*-intercept	r^2	$t_{(0.05(1),\ 14)}$	*p*
QM–PO force$_Y$ (N)	SL	2	2.55	−2.35	0.915	2.654	**0.009**
PO-α force$_Y$ (N)	SL	2	2.44	−2.77	0.813	1.408	0.090
QM-γ force$_Y$ (N)	SL	2	3.41	−4.92	0.759	2.756	**0.008**
QM-PO force$_Y$ (N)	HH	2	2.12	0.11	0.872	0.533	0.301
PO-α force$_Y$ (N)	HH	2	1.96	−0.37	0.727	−0.128	0.550
QM-γ force$_Y$ (N)	HH	2	2.73	−1.57	0.676	1.458	0.083
QM–PO CSA (cm^2)	HW	2	2.25	−1.61	0.955	1.942	**0.036**
PO-α CSA (cm^2)	HW	2	2.00	−2.03	0.825	−0.016	0.506
QM-γ CSA (cm^2)	HW	2	2.23	−2.41	0.852	0.931	0.194

CSA = cross-sectional area; HH = head height; HW = head width; SL = standard length.
All initial regressions from which slopes, *y*-intercepts, and r^2 values were obtained were significant at $p \leq 0.001$. Bold numbers indicate statistically significant *p*-values.

consuming *S. purpuratus* and hard prey with similar material properties very early in its life history (Fig. 4).

At maximum size (93 cm SL) *H. francisci* is capable of consuming *S. purpuratus* of up to 3.56 and 5.98 cm test height with its anterior and posterior bite forces, respectively (Fig. 4). The former of these numbers represents the potential to consume 82% of the size range of *S. purpuratus* (0.6–4.2 cm test height), while the latter is considerably beyond the largest of the urchin size range. The largest *S. purpuratus* (4.2 cm test height) could theoretically be consumed using posterior biting in a 60 cm SL *H. francisci* (Fig. 4), again provided that gape is not a limiting factor.

Regressions of anterior gape and predicted urchin height (based on theoretical anterior bite force) vs. standard length suggest that anterior gape does not constrain consumption of *S. purpuratus* by *H. francisci*. Both the slope ($t_{(2),28} = 3.081$, $p = 0.002$) and *y*-intercept ($t_{(2),29} = 660.960$, $p < 0.001$) of the gape regression were significantly higher than those of predicted urchin height (Fig. 5). These regressions intersect at approximately 4.3 cm SL, considerably prior to the hatchling size of *H. francisci* (13 cm SL), suggesting that anterior gape does not limit consumption of *S. purpuratus* at any point in its life history. Conversely, comparison of posterior gape and predicted urchin height (based on theoretical posterior bite force) relative to standard length does indicate a gape constraint. While the slopes of these regressions were equivalent ($t_{(2),29} = 1.086$, $p = 0.143$), the *y*-intercept of predicted urchin height for posterior biting was significantly higher than that of posterior gape ($t_{(2),29} = 51.327$, $p < 0.001$) (Fig. 5). Consequently, *H. francisci* cannot utilize its high posterior bite force to consume *S. purpuratus* until its posterior gape reaches a minimum of 0.6 cm at 23 cm SL.

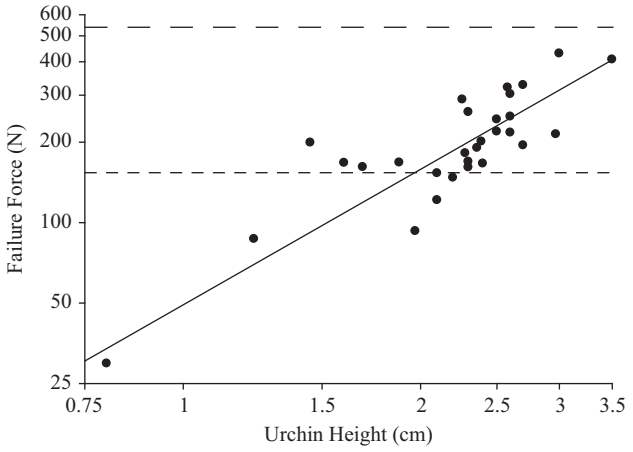

Fig. 3. Forces at which urchin tests underwent catastrophic failure with respect to urchin height in *S. purpuratus* plotted on logarithmic axes (log failure force = 1.69 log urchin height − log 1.70). Small- and large-dashed horizontal lines indicate the maximum theoretical anterior bite forces of the sharks in our data set (163 N) and the largest *H. francisci* on record (530 N), respectively. See Table 4 for additional statistical information.

Discussion

Scaling of feeding biomechanics

As *H. francisci* triples in size (19–59 cm SL), its theoretically estimated anterior bite force increases 20-fold (8–163 N), while that for posterior biting increases

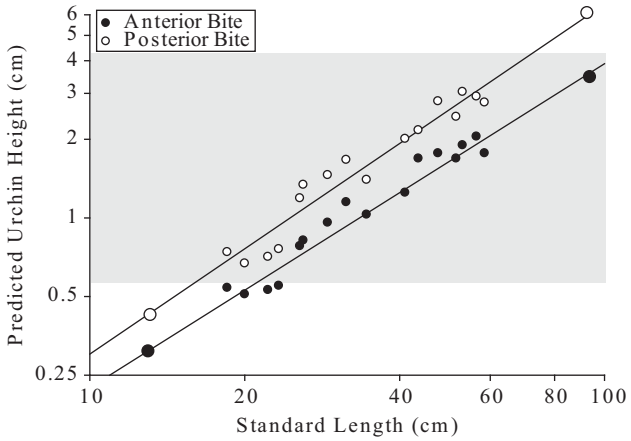

Fig. 4. Maximum height sea urchins that *H. francisci* can consume based upon its theoretical maximum bite force and failure force of *S. purpuratus* with respect to standard length plotted on logarithmic axes (anterior predicted urchin height = 0.04 SL − 0.22, posterior predicted urchin height = 0.06 SL − 0.42). Smaller circles represent predictions for specimens included in this analysis ($n = 16$, 19–59 cm SL). Larger circles marking the endpoints of the data sets represent predictions for the full size range of *H. francisci* (13–93 cm SL). Gray shaded area represents the size range of *S. purpuratus*.

Table 4. Scaling analyses of *S. purpuratus* failure forces with respect to urchin size ($\log y = b \log x + \log a$).

Dependent variable	Independent variable	Isometric slope	Slope	*y*-intercept	r^2	$t_{(0.05(1),\ 28)}$	*P*
Failure force (N)	Test height	2	1.69	1.70	0.788	−1.849	**0.037**
	Test diameter	2	1.66	1.12	0.779	−2.072	**0.034**
	Mass	0.67	0.60	1.31	0.809	−1.353	0.094

All initial regressions from which slopes, *y*-intercepts, and r^2 values were obtained were significant at $p \leq 0.001$. Bold numbers indicate statistically significant *p*-values.

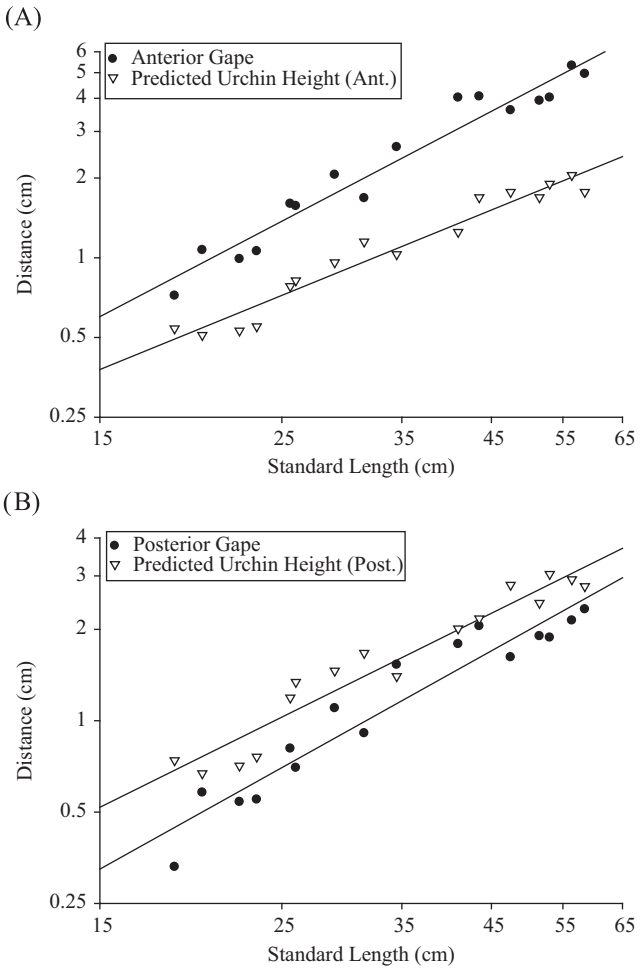

Fig. 5. (A) Anterior gape and maximum height of *S. purpuratus* that *H. francisci* is theoretically capable of consuming based upon theoretical anterior bite force with respect to standard length (SL) (anterior gape = 0.11 SL−1.24, anterior predicted urchin height = 0.04 SL−0.22). (B) Posterior gape and maximum height of *S. purpuratus* that *H. francisci* is theoretically capable of consuming based upon posterior bite force with respect to standard length (SL) (posterior gape = 0.05 SL−0.40, posterior predicted urchin height = 0.06 SL−0.42). Both graphs are plotted on logarithmic axes.

nearly 26 times (15–382 N). Positive allometry of bite force at both points is attributed to allometric increases in the cross-sectional areas of two jaw adducting muscles and mechanical advantage at the posterior bite point. Similar results have been found for the blacktip shark *C. limbatus*, whereas positive allometry of bite force in the spotted ratfish *H. colliei* was attributed to allometric changes in jaw leverage alone (Huber et al., 2006, 2008). Though considerably smaller in size than *C. limbatus*, both *H. francisci* and *H. colliei* generate considerably higher mass-specific bite forces owing to hypertrophied jaw adductors and high-leverage jaw adducting mechanisms. In fact, *H. francisci* and *H. colliei* have among the highest mass-specific bite forces of any cartilaginous fish, which is correlated with hard-prey consumption in both (Huber et al., 2008).

Positive allometry of bite force has now been observed intra-specifically in most vertebrate clades and is often associated with ontogenetic dietary shifts and niche partitioning (Hernandez and Motta, 1997; Herrel et al., 1999; Binder and Van Valkenburgh, 2000; Meyers et al., 2002; Erickson et al., 2003; Herrel and Gibb, 2006; Grubich et al., 2008). While it has traditionally been demonstrated that high bite force leads to niche specialization, only recently has it been shown that high bite forces also increase net energy gain during feeding by increasing prey handling efficiency and facilitating the consumption of large prey relative to predator size (Herrel et al., 2001; Verwaijen et al., 2002; van der Meij et al., 2004). Thus, in the fitness paradigm wherein performance mediates the relationship between morphology and ecology (Arnold, 1983), the selective pressure for high-performance biting is apparent. Interestingly, however, Huber et al. (2009) identified isometric scaling of bite force in a phylogenetically informed analysis of 10 species of sharks spanning three orders of magnitude in length. Interspecific isometry was attributed to a lack of selection for high size-specific biting performance in large megacarnivorous species with high absolute bite forces such as the great hammerhead *Sphyrna mokarran* (2432 N) and the bull shark *Carcharhinus leucas* (1023 N). Presumably the large size of these taxa facilitates high bite forces in the absence of musculoskeletal allometry, whereas smaller taxa may be dependent on allometric growth to surpass the performance thresholds of functionally difficult prey. Further phylogenetic analyses are needed to determine whether positive allometry of bite force is evolutionarily correlated with body size and/or diet among cartilaginous fishes.

Cranial morphometrics

Head width is generally the most accurate predictor of bite force in vertebrates, as it approximates the cross-sectional area available for jaw adducting muscles (Herrel et al., 2005; Brecko et al., 2008; Huber et al., 2009). While this was the case for anterior bite force in *H. francisci*, all cranial morphometrics can be used to accurately predict its biting performance, providing a convenient morphological proxy for rapid estimation of bite force in additional specimens. Posterior bite force was most strongly correlated with head height, which exhibited an isometric relationship with the vertical (*Y*-axis) components of the adductive muscle force vectors. Both head height and these vertical force components were hyperallometric with respect to standard length, suggesting vertical orientation and

growth of the jaw adductors relative to the lower jaw play a key role in the generation of high bite forces in *H. francisci*, in addition to head width. Ontogenetic changes in fiber orientation within these muscles may influence force generation as well (Huber et al., 2008). Positive allometry of cross-sectional area in the primary jaw adductor (QM–PO) relative to head width suggests that the jaws become relatively narrower over ontogeny, which may have consequences for their mechanical function and represents an area for further study on spatial and mechanical developmental constraints in the feeding mechanism of *H. francisci*.

Ontogenetic constraints on feeding ecology

Anterior bite force capacity limits the consumption of hard prey such as *S. purpuratus* early in the life history of *H. francisci*. Juveniles must reach 21 cm SL in order to generate bite forces high enough to crush *S. purpuratus* tests with an anterior bite, which is consistent with observations of hatchlings and juveniles foraging on polychaete worms and sea anemones despite the availability of urchins (Strong, 1989). The juvenile growth rate of closely related Port Jackson sharks *Heterodontus portjacksoni* is 5–6 cm per year (McLaughlin and O'Gower, 1971) suggesting that *H. francisci* can begin consuming urchin-like hard prey using anterior biting during its second year of life. Thereupon the development of anterior bite force allows *H. francisci* to consume successively larger portions of the *S. purpuratus* population. At its maximum size (93 cm SL), *H. francisci* can consume *S. purpuratus* of up to 3.56 cm test height, representing 82% of the available prey population. Anterior gape does not constrain the consumption of *S. purpuratus*, as it is larger than the maximum-size urchins *H. francisci* can consume based upon anterior biting capacity at any point in its life history. This lack of constraint is aided by positive allometry of anterior gape.

Although posterior bite force is sufficient to begin consuming *S. purpuratus* at 17 cm SL, posterior gape does not reach the minimum test height of *S. purpuratus* (0.6 cm) until 23 cm SL. Throughout its entire life history the posterior gape of *H. francisci* limits it to the consumption of urchins that are 43% smaller than its posterior bite force capacity would permit. For the largest specimens in our data set this corresponds to *S. purpuratus* of up to 1.73 cm test height (31% of the available prey population), whereas the largest *H. francisci* (93 cm SL) can consume urchins of up to 3.04 cm test height (78% of the available prey population). Posterior gape was only 7% larger than the maximum-height *S. purpuratus* that can be consumed with an anterior bite based on biomechanical capacity, indicating that posterior biting offers little advantage over anterior biting despite a two-fold increase in leverage between the anterior and posterior bite points and a 2.3-fold increase in bite force. If posterior gape had not scaled with positive allometry, the benefits of increased leverage and bite force at the posterior bite point may have been fully nullified by this gape constraint. This represents considerable pressure for high-performance anterior biting and perhaps a further rationale for hyperallometric bite force.

Urchins that are reduced in height by anterior biting can be transported to posterior bite points at which higher leverage and bite force will more efficiently process fragmented prey (Strong, 1989; Edmonds et al., 2001). Additionally, the posterior gape of *H. francisci* may be large enough to accommodate molluscan taxa with smaller dimensions than *S. purpuratus*, such as dorso-ventrally compressed fissurellid limpets and pelecipod clams and mussels commonly consumed by *H. francisci*, thereby allowing its high posterior biting performance to be utilized. However, blue crabs *Callinectes* spp. commonly consumed by *H. francisci* can grow to carapace heights of approximately 5 cm (Segura-Zarzosa et al., 1997; Atar and Secer, 2003; Mara et al., unpublished data); blue crab consumption by *H. francisci* is likely affected by gape in a manner comparable to that of urchin consumption.

Durophagy in cartilaginous fishes

Positive allometry of bite force has now been identified in both species of durophagous cartilaginous fishes that have been investigated, *H. francisci* and *H. colliei*. While hyperallometric bite force appears to be a general vertebrate phenomenon, it undoubtedly facilitates access to the durophagous trophic niche earlier in life history than alternative ontogenetic trajectories. While additional scaling studies are needed on the other independent evolutionary acquisitions of durophagy among cartilaginous fishes, the present findings suggest that positive allometry of biting performance may complement morphological adaptations including robust, high-leverage jaws, molariform dentition, and hypertrophied jaw adductors in their consumption of hard prey (Summers, 2000; Huber et al., 2005, 2008). Additional *in vivo* biting performance trials are needed in these taxa to identify commonalities in bite force application behaviors as well.

Conclusions

Scaling of feeding performance plays a key role in determining the potential trophic niches of vertebrates, which can subsequently influence resource partitioning and community structure. Over an individual's

ontogeny, positive allometry of feeding performance expands potential trophic niches by accelerating the rate at which additional prey resources can be accessed, increases the efficiency of trophic energy expenditure, and in the case of functionally difficult prey (hard, tough, large, etc.), reduces competition with sympatric species having lower performance capacities. Consequently, positive allometry of bite force in *H. francisci* facilitates entry into the durophagous niche early in its life history and gives it access to nearly the entire *S. purpuratus* population by the time it reaches maximum size. Hyperallometric anterior bite force is particularly relevant given that processing prey at the force-efficient posterior margin of the jaws is significantly constrained by gape. Lastly, the ontogenetic relationship between muscle geometry and cranial dimensions underscores the importance of analyzing muscle position and structure in addition to size in studies of organismal performance.

Acknowledgements

This work is dedicated to the memory of G. Rau for inspiring a spirit of discovery and nurturing all fascinations, no matter how bizarre.

We would like to thank the Biology Departments of the University of Tampa and the University of South Florida, as well as the Harvard University Museum of Comparative Zoology, Canadian Museum of Nature, C. Lowe, and D. Pondella for specimen donations and loans. Material testing of sea urchins was made possible by the University of South Florida College of Engineering with the help of L. Whitenack, K. Mara, K. Campbell, J. Pfeiffenberger, and P. Motta. Funding for this project was provided by the University of Tampa, University of South Florida Presidential Research Fellowship to DRH, and an independent research stipend from the University of Tampa College of Natural and Health Sciences to MAK.

Appendix A. Supporting Information

Supplementary data associated with this article can be found in the online version at doi:10.1016/j.zool.2008.11.002.

References

Aguirre, L.F., Herrel, A., Van Damme, R., Matthysen, E., 2003. The implications of food hardness for diet in bats. Funct. Ecol. 17, 201–212.

Arnold, S.J., 1983. Morphology, performance, and fitness. Am. Zool. 23, 347–361.

Atar, H.H., Secer, S., 2003. Width/length–weight relationships of the blue crab (*Callinectes sapidus* Rathbun 1896) population living in Beymelek Lagoon Lake. Turk. J. Vet. Anim. Sci. 27, 443–447.

Binder, W.J., Van Valkenburgh, B.V., 2000. Development of bite strength and feeding behavior in juvenile spotted hyenas (*Crocuta crocuta*). J. Zool. 252, 273–283.

Brecko, J., Huyghe, K., Vanhooydonck, B., Herrel, A., Grbac, I., Van Damme, R., 2008. Functional and ecological significance of intraspecific variation in body size and shape in the lizard *Podarcis melisellensis* (Lacertidae). Biol. J. Linn. Soc. 94, 251–264.

Clifton, K.B., Motta, P.J., 1998. Feeding morphology, diet, and ecomorphological relationships among five Caribbean labrids (Teleostei, Labridae). Copeia 1998, 953–966.

Compagno, L.J.V., 2001. Sharks of the World, vol. 2. Bullhead, Mackerel, and Carpet Sharks (Heterodontiformes, Lamniformes, and Orectolobiformes). Food and Agriculture Organization of the United Nations, Rome.

Currey, J.D., 1980. Mechanical properties of mollusc shell. In: Vincent, J.F.V., Currey, J.D. (Eds.), The Mechanical Properties of Biological Materials. Press Syndicate of the University of Cambridge, Cambridge, pp. 75–98.

Ebert, T.A., 1968. Growth rates of the sea urchin *Strongylocentrotus purpuratus* related to food availability and spine abrasion. Ecology 49, 1075–1091.

Edmonds, M.A., Motta, P.J., Hueter, R.E., 2001. Food capture kinematics of the suction feeding horn shark *Heterodontus francisci*. Environ. Biol. Fish. 62, 415–427.

Erickson, G.M., Lappin, A.K., Vliet, K.A., 2003. The ontogeny of bite-performance in American alligator (*Alligator mississippiensis*). J. Zool. 260, 317–327.

Grubich, J.R., Rice, A.N., Westneat, M.W., 2008. Functional morphology of bite mechanics in the great barracuda (*Sphyraena barracuda*). Zoology 111, 16–29.

Hernandez, L.P., Motta, P.J., 1997. Trophic consequences of differential performance: ontogeny of oral jaw-crushing performance in the sheepshead, *Archosargus probatocephalus* (Teleostei, Sparidae). J. Zool. 243, 737–756.

Herrel, A., Gibb, A.C., 2006. Ontogeny of performance in vertebrates. Physiol. Biochem. Zool. 79, 1–6.

Herrel, A., O'Reilly, J.C., 2006. Ontogenetic scaling of bite force in lizards and turtles. Physiol. Biochem. Zool. 79, 31–42.

Herrel, A., Spithoven, L., Van Damme, R., De Vree, F., 1999. Sexual dimorphism of head size in *Gallotia galloti*: testing the niche divergence hypothesis by functional analyses. Funct. Ecol. 13, 289–297.

Herrel, A., Van Damme, R., Vanhooydonck, B., De Vree, F., 2001. The implications of bite force for diet in two species of lacertid lizards. Can. J. Zool. 79, 662–670.

Herrel, A., Podos, J., Huber, S.K., Hendry, A.P., 2005. Evolution of bite force in Darwin's finches: a key role for head width. J. Evol. Biol. 18, 669–675.

Huber, D.R., Eason, T.G., Hueter, R.E., Motta, P.J., 2005. Analysis of the bite force and mechanical design of the feeding mechanism of the durophagous horn shark *Heterodontus francisci*. J. Exp. Biol. 208, 3553–3571.

Huber, D.R., Weggelaar, C.L., Motta, P.J., 2006. Scaling of bite force in the blacktip shark *Carcharhinus limbatus*. Zoology 109, 109–119.

Huber, D.R., Dean, M.N., Summers, A.P., 2008. Hard prey, soft jaws, and the ontogeny of feeding biomechanics in the spotted ratfish *Hydrolagus colliei*. J. Roy. Soc. Int. 5, 941–952.

Huber, D.R., Claes, J.M., Mallefet, J., Herrel, A., 2009. Is extreme bite performance associated with extreme morphologies in sharks? Physiol. Biochem. Zool. 82, 20–28.

Keast, A., 1985. Development of dietary specialization in a summer community of juvenile fishes. Environ. Biol. Fish. 13, 211–224.

Kiltie, R.A., 1982. Bite force as a basis for niche diversification between rain forest peccaries (*Tayassu tajacu* and *T. pecari*). Biotropica 14, 188–195.

Korff, W.L., Wainwright, P.C., 2004. Motor pattern control for increasing crushing force in the striped burrfish (*Chilomycterus schoepfi*). Zoology 107, 335–346.

Lou, F., Curtin, N.A., Woledge, R.C., 2002. Isometric and isovelocity contractile performance of red muscle fibers from the dogfish *Scyliorhinus canicula*. J. Exp. Biol. 205, 1585–1595.

McLaughlin, R.H., O'Gower, A.K., 1971. Life history and underwater studies of a heterodont shark. Ecol. Monogr. 41, 271–289.

Meyers, J.J., Herrel, A., Birch, J., 2002. Scaling of morphology, bite force and feeding kinematics in an iguanian and scleroglossan lizard. In: Aerts, P., D'Aout, K., Herrel, A., Van Damme, R. (Eds.), Topics in Functional and Ecological Vertebrate Morphology. Shaker Publishing, Netherlands, pp. 47–62.

Morris, R.H., Abbott, D.P., Haderlie, E.C., 1980. Intertidal Invertebrates of California. Stanford University Press, Palo Alto, CA.

Segura-Zarzosa, J.C., Abitia-Cardenas, L.A., Galvan-Magana, F., 1997. Observations on the feeding habits of the shark *Heterodontus francisci* Girard 1854 (Chondrichthyes: Heterodontidae), in San Ignacio Lagoon, Baja California Sur, Mexico. Cienc. Mar. 23, 111–128.

Strong Jr., W.R., 1989. Behavioral ecology of horn sharks, *Heterodontus francisci*, at Santa Catalina Island, California, with emphasis on patterns of space utilization. M.S. Thesis, California State University, Long Beach, CA.

Summers, A.P., 2000. Stiffening the stingray skeleton: an investigation of durophagy in myliobatid stingrays (Chondrichthyes, Batoidea, Myliobatidae). J. Morphol. 243, 113–126.

Summers, A.P., Long Jr., J.H., 2006. Skin and bones, sinew and gristle: the mechanical behavior of fish skeletal tissues. In: Shadwick, R.E., Lauder, G.V. (Eds.), Fish Biomechanics. Elsevier Academic Press, San Diego, CA, pp. 141–178.

van der Meij, M.A.A., Griekspoor, M., Bout, R.G., 2004. The effect of seed hardness on husking time in finches. Anim. Biol. 54, 195–205.

Verwaijen, D., Van Damme, R., Herrel, A., 2002. Relationships between head size, bite force, prey handling efficiency and diet in two sympatric lacertid lizards. Funct. Ecol. 16, 842–850.

Wainwright, P.C., 1987. Biomechanical limits to ecological performance: mollusc-crushing by the Caribbean hogfish, *Lachnolaimus maximus* (Labridae). J. Zool. 213, 283–297.

Wainwright, P.C., 1988. Morphology and ecology: functional basis of feeding constraints in Caribbean labrid fishes. Ecology 69, 635–645.

Wainwright, S.A., Biggs, W.D., Currey, J.D., Gosline, J.M., 1976. Mechanical Design in Organisms. Princeton University Press, Princeton, NJ.

Wilga, C.D., Motta, P.J., 2000. Durophagy in sharks: feeding mechanics of the hammerhead *Sphyrna tiburo*. J. Exp. Biol. 203, 2781–2796.

Wroe, S., Huber, D.R., Lowry, M., McHenry, C., Moreno, K., Clausen, P., Ferrara, T., Cunningham, E., Dean, M.N., Summers, A.P., 2008. Three-dimensional computer analysis of white shark jaw mechanics: how hard can a great white bite? J. Zool. 276, 336–342.

Wyckmans, M., Van Wassenburgh, S., Adriaens, D., Van Damme, R., Herrel, A., 2007. Size-related changes in cranial morphology affect diet in the catfish *Clariallabes longicauda*. Biol. J. Linn. Soc. 92, 323–334.